AMERICAN SOCIETY FOR MICROBIOLOGY | Infection and Immunity®

BACTERIAL INFECTIONS

Coxiella burnetii Plasmid Effector B Promotes LC3-II Accumulation and Contributes To Bacterial Virulence in a SCID Mouse Model

Mengjiao Fu,[a] Jianing Zhang,[a] Mingliang Zhao,[a] Shan Zhang,[a] Lupeng Dai,[a,b] Xuan Ouyang,[a] Yonghui Yu,[a] Bohai Wen,[a] Dongsheng Zhou,[a] Yansong Sun,[a] Jun Jiao,[a] Xiaolu Xiong[a]

[a]State Key Laboratory of Pathogen and Biosecurity, Beijing Institute of Microbiology and Epidemiology, Fengtai, Beijing, People's Republic of China
[b]Anhui Medical University, Hefei, Anhui, China

Mengjiao Fu and Jianing Zhang contributed equally to this article. Author order was determined on the basis of seniority.

ABSTRACT *Coxiella burnetii*, the causative agent of zoonotic Q fever, is characterized by replicating inside the lysosome-derived *Coxiella*-containing vacuole (CCV) in host cells. Some effector proteins secreted by *C. burnetii* have been reported to be involved in the manipulation of autophagy to facilitate the development of CCVs and bacterial replication. Here, we found that the *Coxiella* plasmid effector B (CpeB) localizes on vacuole membrane targeted by LC3 and LAMP1 and promotes LC3-II accumulation. Meanwhile, the *C. burnetii* strain lacking the QpH1 plasmid induced less LC3-II accumulation, which was accompanied by smaller CCVs and lower bacterial loads in THP-1 cells. Expression of CpeB in the strain lacking QpH1 led to restoration in LC3-II accumulation but had no effect on the smaller CCV phenotype. In the severe combined immune deficiency (SCID) mouse model, infections with the strain expressing CpeB led to significantly higher bacterial burdens in the spleen and liver than its parent strain devoid of QpH1. We also found that CpeB targets Rab11a to promote LC3-II accumulation. Intratracheally inoculated *C. burnetii* resulted in lower bacterial burdens and milder lung lesions in Rab11a conditional knockout (Rab11a$^{-/-}$ CKO) mice. Collectively, these results suggest that CpeB promotes *C. burnetii* virulence by inducing LC3-II accumulation via a pathway involving Rab11a.

KEYWORDS *Coxiella burnetii*, Q fever, CpeB, Rab11a, autophagy

Coxiella burnetii, the causative agent of zoonotic Q fever, is an intracellular Gram-negative bacterium characterized by proliferating in lysosome-derived vacuoles in host cells (1–3). *C. burnetii* infection usually causes flulike acute respiratory infections, as well as chronic and persistent infections, with endocarditis, hepatitis, osteomyelitis, etc., as the main symptoms (4). Following uptake by a susceptible host cell, *C. burnetii* traffics through the phagolysosomal maturation pathway to complete the colonization (5). Phagosomes containing *C. burnetii* consecutively fuse with autophagosomes, lysosomes, and endocytic vesicles to develop *Coxiella*-containing vacuoles (CCVs) (2, 5–7). The internal environment of mature CCV is acidic and contains a variety of active lysosomal-derived proteases. Different from other intracellular bacteria, *C. burnetii* can efficiently translocate its effector proteins into the host cell cytoplasm via its Dot/Icm type IV secretion system (T4SS) in this acidic environment (8, 9). More than 150 T4SS substrates of *C. burnetii* have been predicted, but most of them need to be further confirmed as bona fide T4SS-secreted effectors (9–11). Some of these effector proteins are highly expressed during the formation and maturation stages of CCVs and participate in a variety of physiological processes of host cells (12). Due to the constraints of

Editor Craig R. Roy, Yale University School of Medicine

Address correspondence to Xiaolu Xiong, xiongxiaolu624@sohu.com, Jun Jiao, jiaojun51920@sina.com, or Yansong Sun, sunys1964@hotmail.com.

The authors declare no conflict of interest.

Received 9 January 2022
Returned for modification 14 February 2022
Accepted 2 May 2022
Published 19 May 2022

genetic manipulation in *C. burnetii* organisms, the function of the majority of these identified effector proteins remains undefined.

Autophagy is a eukaryotic process of degradation and recycling damaged cellular components and is also an important way for host cells to resist infection and maintain their own homeostasis. In the course of *C. burnetii* infection, autophagosomes are recruited to the CCV, and host lipoprotein LC3-II protein levels increase, with the level of p62 remaining unchanged (13, 14), and the autophagosome markers (LC3, Rab24, etc.) are embedded on the CCV membrane (15, 16). With the expansion of CCV, endogenous LC3-II continues to accumulate on its lumen membrane, indicating that the fusion between the CCV and LC3-labeled autophagosomes persists during infection (17). Meanwhile, inhibition of autophagy-related components results in defects in homotypic fusion of CCVs in host cells (18, 19).

In the context of *C. burnetii* infection, several members of the Rab GTPase family are required for vesicular trafficking and membrane fusion. Rab5 is located on the phagosomes containing *C. burnetii* and promotes CCV fusion with early endosomes. Next, Rab7 promotes the CCV fusion with late endosomes (20, 21). In addition to Rab5 and Rab7, Rab1b, Rab24, and Rab26 are recruited to the membrane of CCVs at different stages after infection and affect vacuole biogenesis and intracellular *C. burnetii* replication (17, 20, 22, 23). Rab11a is a marker for recycling endosomes and regulates vesicle trafficking by recycling early endosomes and endosome-like structures. Recent studies have shown that the membrane structure labeled with Rab11a receives membrane structures from sources such as the endoplasmic reticulum, recycled endosomes, Golgi apparatus, and cell membranes and mediates the formation and maturation of autophagosomes (24). As the main direct platform for the formation of classic autophagosomes, the role of Rab11a in *C. burnetii* infection remains unrevealed.

All *C. burnetii* isolates carry a large, autonomously replicating plasmid or have chromosomally integrated plasmid-like sequences, and QpH1 is the best-studied plasmid (25–28). *Coxiella* plasmid effector B (CpeB, CBUA0013) is highly conserved in all *C. burnetii* plasmids. An earlier study revealed that maximal expression of CpeB occurred at the early log phase of infection. Moreover, CpeB colocalizes with LC3 on autophagosomes (29). Although a number of effectors encoded by plasmids have been identified, their function and roles in *C. burnetii* virulence remain mostly unknown.

With the development of genetic manipulation methodology and the application of animal infection models, the function of effector proteins, and the mechanisms underlying host-pathogen interactions will be gradually clarified. Here, we demonstrated that CpeB interacts with host Rab11a and induces LC3-II accumulation during *C. burnetii* infection. Expression of CpeB in the QpH1-deficient strain restored the bacterial virulence in a SCID mouse infection model. We also found that CpeB targeted Rab11a, which was required for maximal virulence.

RESULTS

CpeB promotes the accumulation of LC3-II and colocalizes on the membrane of CCVs. Although the close relationship between autophagy and intracellular *C. burnetii* replication has been verified (15), several studies have also shown that knockdown of autophagy-related essential genes with small interfering RNAs (siRNAs) leads to the formation of multiple small vacuoles but does not affect intracellular *C. burnetii* replication (6). In this study, THP-1 cells were infected with the Nine Mile phase II (NMII) strain, and then the modification of cellular pathway-related markers was analyzed by Western blotting. Compared with that of the uninfected group, phosphorylation of p65 and Akt presented a transient increase and then returned to normal levels, while the level of p-p38 showed no significant difference except for a slight increase in *C. burnetii*-infected cells. Moreover, *C. burnetii* infection triggered a steadily higher level of LC3-II in host cells (Fig. 1A; see Fig. S2A in the supplemental material). Meanwhile, the treatment of rapamycin increased the intracellular *C. burnetii* replication, and bafilomycin A1 inhibited the proliferation of *C. burnetii* in a dose-dependent manner (Fig. 1B). Subcellular location analysis revealed that ectopically expressed CpeB exhibits

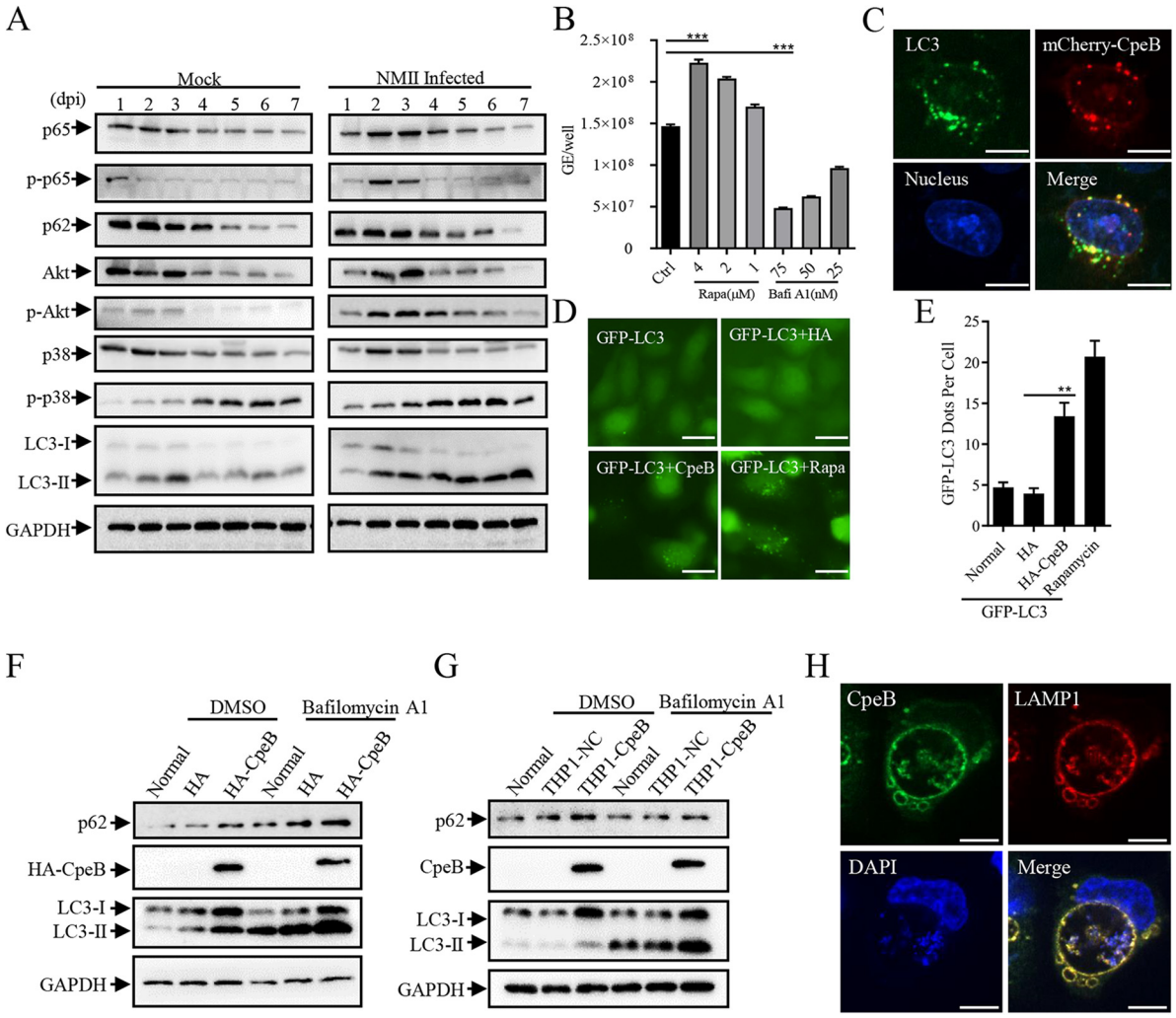

FIG 1 CpeB promotes the accumulation of LC3 and colocalizes on the membrane of CCVs. (A) THP-1 cells were infected with *C. burnetii* at an MOI of 10. At different time points (1, 2, 3, 4, 5, 6, and 7 days) postinfection, cells were lysed, and the expression of different markers, including p65/p-p65, Akt/p-Akt, p38/p-p38, p62, and LC3, was detected by Western blotting. GAPDH expression was used as an internal control. (B) Differentiated THP-1 cells (1×10^6 cells/mL) were treated with rapamycin or bafilomycin A1 at the indicated concentration for 48 h after infection. Genome equivalents of *C. burnetii* were quantitated by qPCR at 5 days postinfection. All samples were carried out in triplicate on the same plate. (C) HeLa cells were transfected with mCherry-CpeB. Twenty-four hours later, cells were fixed, and endogenous LC3 was labeled with an anti-LC3 antibody. The colocalization of LC3 and CpeB was observed with a Nikon Eclipse Ti microscope (magnifications, ×600; bar, 10 μm). (D) HeLa cells were transfected with pEGFP-LC3 alone (normal) or cotransfected with pCMV-HA (HA) or pCMV-HA-CpeB (HA-CpeB). Rapamycin (4 μM) was used as a positive control. (E) Twenty-four hours later, the GFP-LC3 dots were observed under a fluorescence microscope (magnification, ×200; bar, 20 μm), and the number of GFP-LC3 dots per cell (n = 20) was counted. (F) HeLa cells were transfected with pCMV-HA or pCMV-CpeB. Twenty-four hours later, cells were treated with bafilomycin A1 (50 nM) or dimethyl sulfoxide (DMSO) as control for 4 h before being lysed. The expression of LC3, p62, and HA-CpeB was examined using Western blotting. GAPDH was used as an internal control. (G) THP-1, THP1-NC, or THP1-CpeB cells were pretreated with bafilomycin A1 or DMSO before collection, and then the expression of CpeB, LC3, or p62 was detected by Western blotting using anti-CpeB, anti-LC3, or anti-p62 antibodies. (H) THP1-CpeB cells were infected with WT *C. burnetii* at the MOI of 10. Four days postinfection, cells were fixed and labeled with anti-CpeB (green) and anti-LAMP1 (red) antibodies. Nucleic acid was stained with DAPI (blue) (magnification, ×600; bar, 10 μm). Data are representative of three independent experiments, and bars represent the mean ± SD of three independent experiments. Significances are represented as follows: ***, $P < 0.001$; **, $P < 0.01$; and *, $P < 0.05$.

point-like aggregation and colocalizes with LC3 in HeLa cells (Fig. 1C). Similarly, coexpression of HA-CpeB and GFP-LC3 resulted in significant aggregation compared with the expression of GFP-LC3 in HeLa cells (Fig. 1D and E). Using Western blotting to detect the effect of CpeB on LC3 expression, it was found that ectopically expressed CpeB increased the level of LC3-II with or without bafilomycin A1 treatment (Fig. 1F and G and Fig. S2B and C). Furthermore, CpeB colocalized with LAMP1 on the membrane of CCVs in *C. burnetii*-infected THP1-CpeB cells (Fig. 1H). Collectively, these

results indicated that CpeB promotes LC3-II accumulation and might play a role in CCV biogenesis.

Expression of CpeB in QpH1-deficient strain restores the decreased LC3-II level. Based on the principle of incompatibility of similar plasmids, shuttle vectors (pQGK, pQGK-CpeA, pQGK-CpeB, and pQGK-CpeC) containing *cbua0036-0039a* and RSF1010-ori were constructed as described above, and the various *C. burnetii* mutants were generated via transformation of the corresponding shuttle plasmids into the wild-type *C. burnetii* strain (NMII). The individual transformant of these mutant strains on ACCM-2 agar plates was shown in Fig. 2A, and the successful construction was verified using reverse transcription-quantitative PCR (qRT-PCR) by examining the expression of *cpeA*, *cpeB*, or *cpeC* mRNA (Fig. S3A to C). After 7 days of continuous cultivation in ACCM-2 and daily sampling, no significant difference in the *in vitro* growth was found among these mutant strains by qPCR assay (Fig. S3D). In infected THP-1 cells, the intracellular growth ability of the NMII*pQGK* mutant was lower than that of NMII, but expression of CpeB in the NMII*pQGK* mutant (NMII*pQGK-cpeB*) partially restored the defect in replication of *C. burnetii* in host cells caused by QpH1 deficiency (Fig. 2B). Moreover, NMII*pQGK-cpeB* infection restored the decreased level of LC3-II induced by NMII*pQGK* infection (Fig. 2C and D). In the rapid proliferation period (2, 3, and 4 days postinfection), this difference was even more pronounced. In addition, the amount of LC3 on vacuole membranes formed by NMII*pQGK-cpeB* infection was much higher than that formed by NMII*pQGK* infection (Fig. S4A and B). However, no obvious differences in LC3-II levels were observed between NMII*pQGK-cpeA*- or NMII*pQGK-cpeC*- infected cells and NMII*pQGK*-infected cells (Fig. 2E and Fig. S4C). These results confirmed the irreplaceable role of QpH1 in *C. burnetii* replication and the importance of CpeB in inducing LC3-II accumulation during *C. burnetii* infection.

CpeB cannot rescue the small-vacuole phenotype caused by QpH1 deficiency. CCVs form approximately 8 h after infection and expand drastically via homotypic fusion of multiple smaller CCVs (30, 31). The large CCV continues to expand through fusion with autophagic, endocytic lysosome vesicles and can occupy nearly the entire volume of the host cell (2, 32). Accordingly, the maturation and maintenance of large CCVs are crucial to intracellular *C. burnetii* replication. In the THP-1 cells infected with wild-type (WT) *C. burnetii*, the bacteria gathered in a large vesicle labeled with LAMP1, and the vesicle gradually enlarged with the prolongation of infection time (Fig. 3A). However, in NMII*pQGK*-infected THP-1 cells, numerous small vacuoles were observed (Fig. 3B), and the number of small vacuoles increased, but vacuole fusion did not occur as the infection time prolonged, indicating that some effector proteins encoded by QpH1 plasmid are involved in the development of vacuole fusion. Meanwhile, in THP-1 cells infected with the NMII*pQGK-cpeB* strain, small vacuoles were also observed (Fig. 3C), suggesting that the expression of CpeB could not rescue the small vacuole defect caused by QpH1 deficiency. Likewise, in THP-1 cells infected with NMII*pQGK-cpeA* or the NMII*pQGK-cpeC* mutant, small disintegrated CCVs were also characterized (Fig. 3D and E). Instead of CpeA, CpeB, and CpeC, other effectors on QpH1 plasmid or the combination of multiple effectors might be responsible for the disability of fusion of small vesicles.

CpeB is a potential virulence factor of *C. burnetii*. Due to the inherent resistance of mice to *C. burnetii*, phase II strains could not colonize and would be quickly eliminated in immunocompetent mice (33), making it difficult for phase II strains to establish infection in immunocompetent mice. SCID mice are severely immunodeficient and have been widely used as infection models for identifying virulence determinants in *C. burnetii* strains (34, 35). To further explore whether CpeB is related to *C. burnetii* virulence, SCID mice were infected with the NMII WT strain or the NMII*pQGK* or NMII*pQGK-cpeB* mutant in the present study. WT strain infection caused significant splenomegaly and hepatomegaly in SCID mice compared with those of the uninfected group (Fig. 4A and D). The ratios of spleen weight to body weight and liver weight to body weight in the mice infected with NMII*pQGK* were lower than those in the mice infected with the WT *C. burnetii* strain (Fig. 4B and E), demonstrating that QpH1 is involved in *C. burnetii*

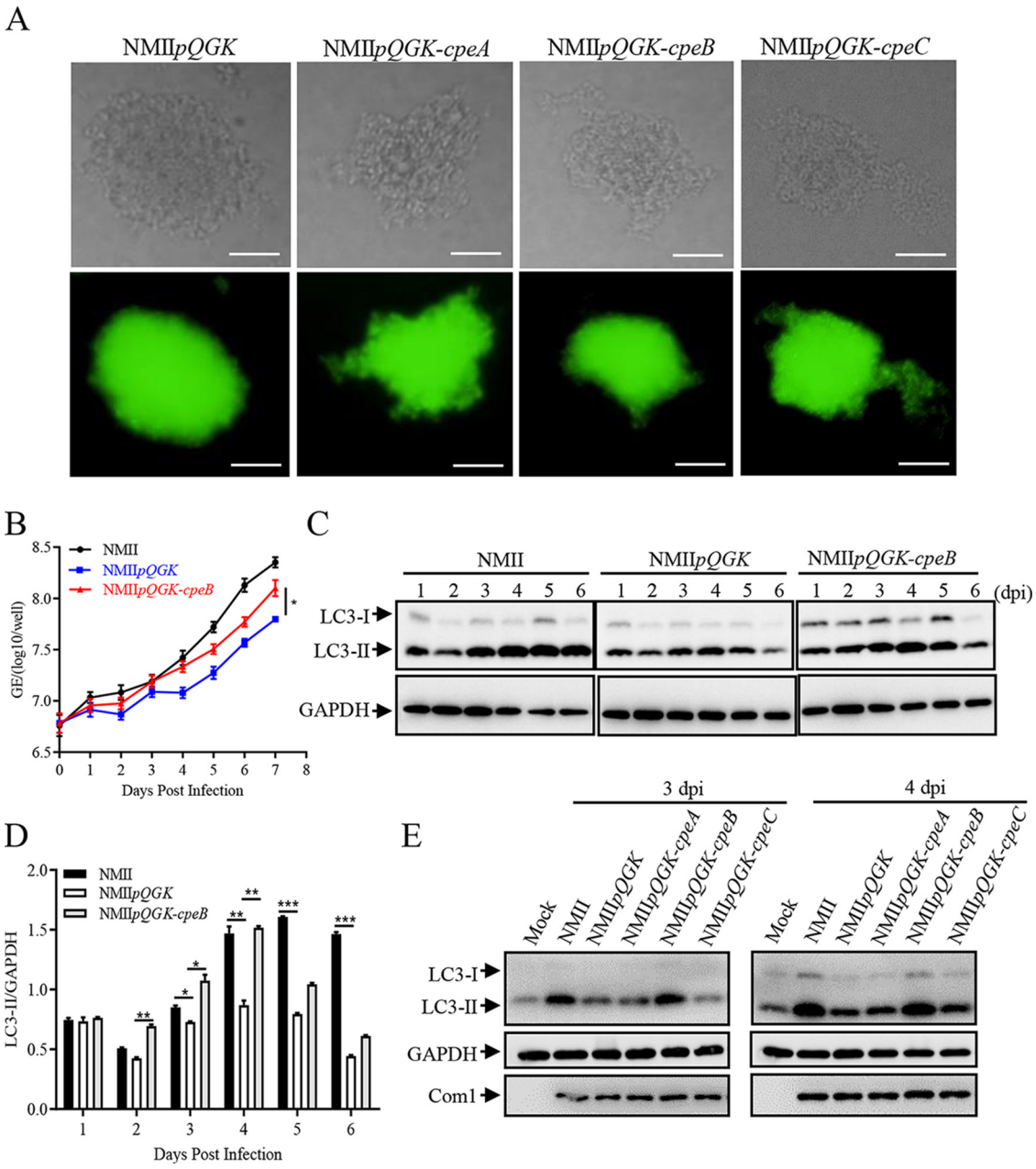

FIG 2 CpeB restores the decreased LC3-II level caused by QpH1 deficiency. (A) Single colonies of different *C. burnetii* mutants on ACCM-2 agar plates were observed under a light microscope (top) and a fluorescence microscope (bottom) at a magnification of ×200. Bar, 20 μm. (B) Differentiated THP-1 cells (1×10^6 cells/mL) were infected with NMII, NMII*pQGK* or NMII*pQGK-cpeB* strains. The genomic DNA of *C. burnetii* was extracted, and the GEs were quantitated by qPCR daily postinfection. Experiments were repeated three times independently, and the trend was consistent. Data are representative of three independent experiments, and bars represent the mean ± SD from three independent experiments ($P < 0.05$). (C) THP-1 cells were infected with NMII, NMII*pQGK*, or NMII*pQGK-cpeB* strains. At indicated times postinfection, cells were lysed, and the expression of LC3 was detected by Western blotting. Endogenous GAPDH was used as an internal control. (D) The band density of LC3-II in panel C was quantitated by densitometry. The relative levels of LC3-II were calculated as follows: band density of LC3-II/band density of GAPDH. Data are representative of three independent experiments, and bars represent the mean ± SD of three independent experiments. ***, $P < 0.001$; **, $P < 0.01$; *, $P < 0.05$. (E) THP-1 cells were mock infected or infected with NMII or different mutant strains at an MOI 0f 10. At day 3 or 4 postinfection, the expression of LC3 was detected. GAPDH was used as an internal control, and *com*1 expression was used as a reference for infection.

pathogenicity. In addition, the ratio of liver weight to body weight in the mice infected with NMII*pQGK-cpeB* was higher than that in the mice infected with NMII*pQGK* (Fig. 4E). Using qPCR to determine *C. burnetii* loads in organs of the infected mice, it was found that the bacterial load in the spleens and livers of the mice infected with the

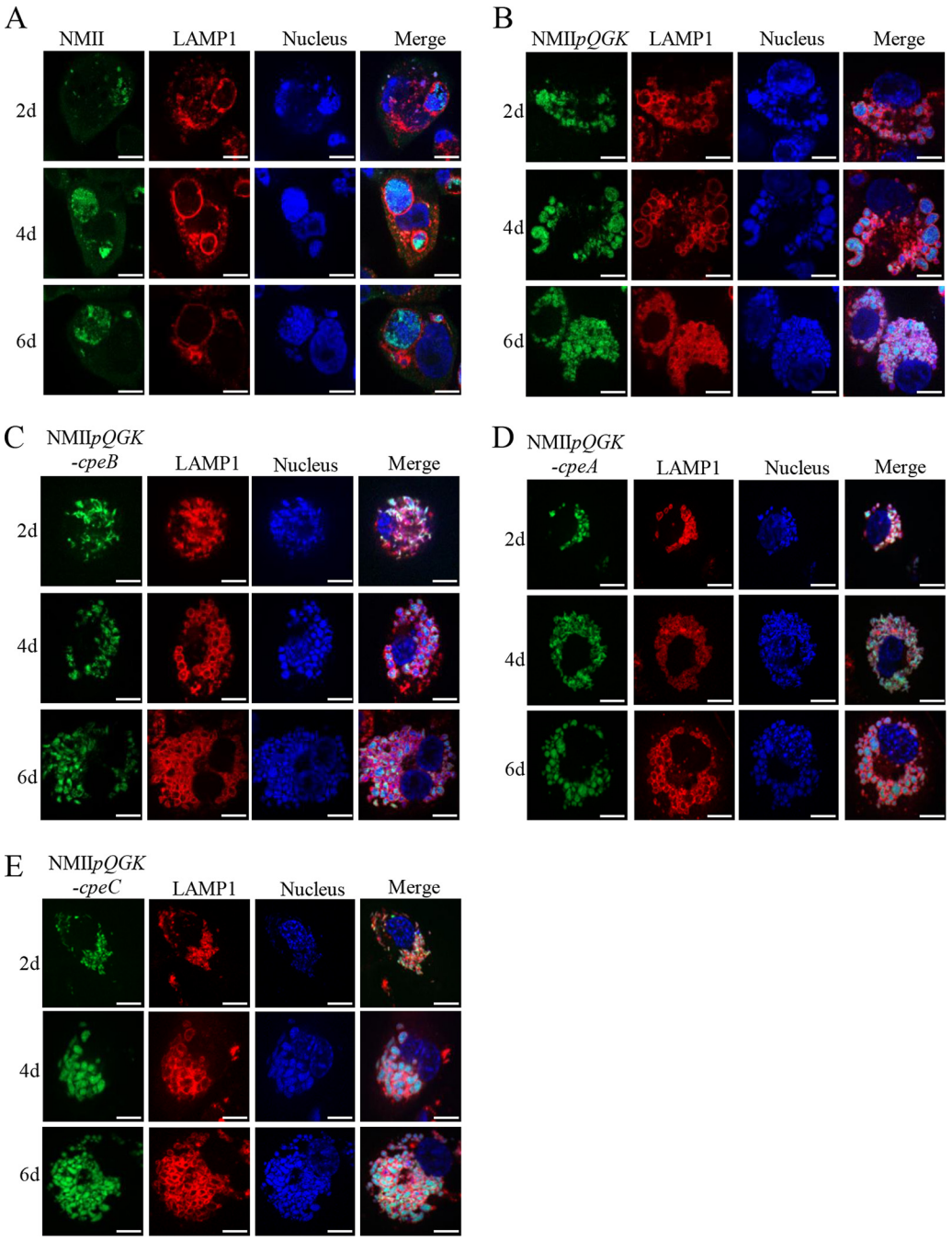

FIG 3 CpeB could not rescue the small-vacuole phenotype caused by QpH1 deficiency. (A to E) THP-1 cells were infected with WT *C. burnetii* or different mutants at an MOI of 100. At different days postinfection, cells were fixed and permeabilized. Membranes of CCV were labeled with anti-LAMP1 antibody followed by the goat anti-rabbit Alexa Fluor 594 antibody (red), and *C. burnetii* was marked by anti-*C. burnetii* serum followed by goat anti-mouse Alexa Fluor 488 antibody (green). Nucleic acid was stained with DAPI (blue). The samples were observed with a laser confocal scanning microscope (magnification, ×600; bar, 10 μm).

NMII*pQGK-cpeB* mutant was markedly lower than that of the mice infected with WT strain, while it was much higher than that of the mice infected with the NMII*pQGK* mutant (Fig. 4C and F). These results indicated that CpeB is a potential *C. burnetii* virulence factor that plays a role in *C. burnetii* pathogenicity in a SCID mouse model.

CpeB interacts with host Rab11a. The host target proteins interacting with effector CpeB were identified by affinity purification-mass spectrometry (AP-MS) (Table S1). Host proteins that were repeatedly pulled down by CpeB in three independent

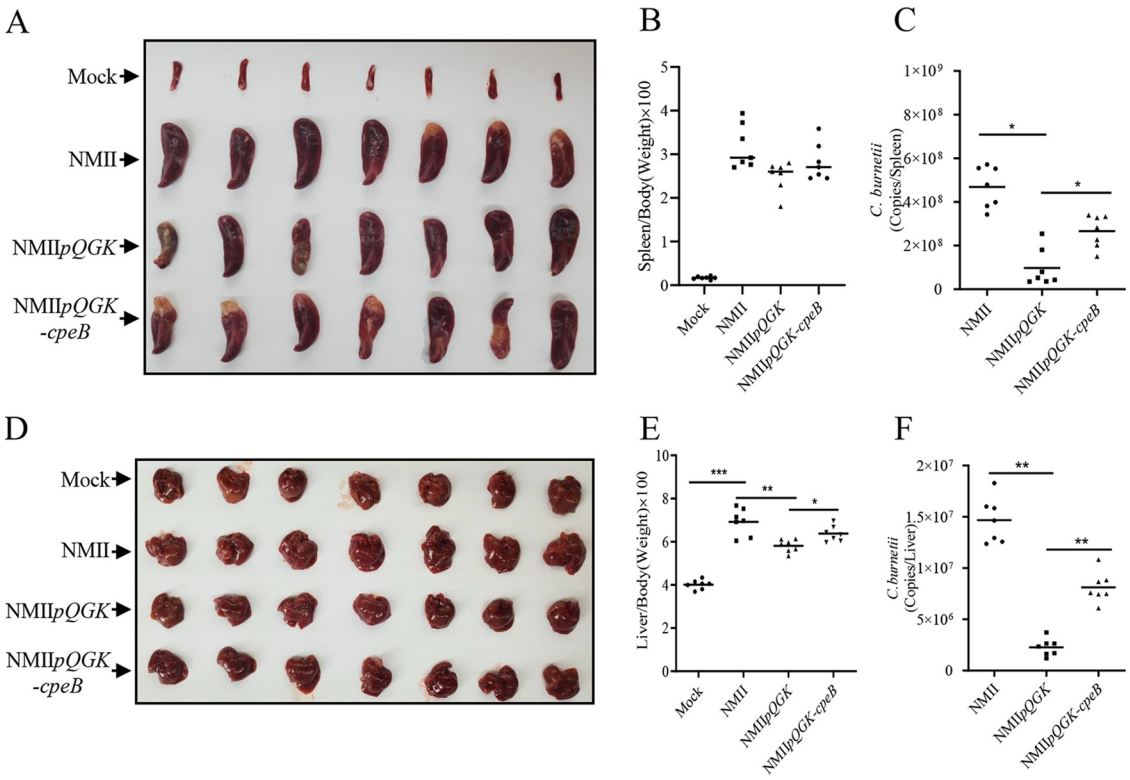

FIG 4 CpeB is related to *C. burnetii* pathogenicity in a SCID mouse model. Two weeks after infection with NMII, NMII*pQGK*, or NMII*pQGK-cpeB*, SCID mice were sacrificed, and the spleens (A) and livers (D) were removed and photographed for comparation. Spleens (B) or livers (E) were weighed, and the ratio of organs to the body of each mouse was calculated. Additionally, the *C. burnetii* genome copies of the spleens (C) or the livers (F) were determined by qPCR. The data are presented as the mean of $n = 7$ mice per group, and the standard error is indicated by the error bar. Significant differences between groups are presented as mean ± SD. ***, $P < 0.001$; **, $P < 0.01$; *, $P < 0.05$.

experiments and could not be pulled down by control proteins were selected as candidates. Among them, Rab11a has been reported to be involved in autophagosome biogenesis by binding WIPI2 and PI3P (24). This reminded us to select Rab11a as the interactor of CpeB for further study. The interaction between CpeB and Rab11a was verified using coimmunoprecipitation (co-IP) in HeLa cells coexpressing Strep-CpeB and FLAG-Rab11a (Fig. 5A) and confocal microscope observation of HeLa cells coexpressing mCherry-CpeB and FLAG-Rab11a (Fig. 5B). Furthermore, coexpressing HA-CpeB and FLAG-Rab11a truncations revealed that CpeB mainly interacts with amino acid residues 1 to 121 of Rab11a (Fig. 5C), and coimmunoprecipitation of FLAG-Rab11a and CpeB truncations revealed that the domain of amino acid residues 164 to 204 of CpeB is sufficient for the interaction with Rab11a (Fig. 5D).

Rab11a affects the intracellular replication of *C. burnetii* through modulating autophagy. To determine whether Rab11a is involved in autophagy and *C. burnetii* intracellular survival in host cells, the replication of *C. burnetii* in host cells transfected with FLAG-Rab11a or rab11a siRNAs was determined by qPCR specific for *C. burnetii*. As a result, the overexpression of Rab11a promoted the intracellular survival of *C. burnetii*, while the replication of *C. burnetii* decreased after interfering with the expression of Rab11a with siRNA (Fig. 6A). Additionally, ectopic expression of Rab11a increased the level of LC3-II with or without the presence of bafilomycin A1 (Fig. 6B and Fig. S5A), while inhibition of Rab11a decreased the levels of LC3-II (Fig. 6C and Fig. S5B). Similarly, the expression of Rab11a promoted the accumulation of LC3-II in HeLa cells (Fig. 6D and E). In addition, compared with control cells, a lower replication level of *C. burnetii* was observed in the THP1-Rab11a-KD cells (Fig. 6F and Fig. S5D and E). To clarify the functional link between CpeB and Rab11a in modulating autophagy, we detected the effect of CpeB on inducing LC3-II accumulation in the case of interfering

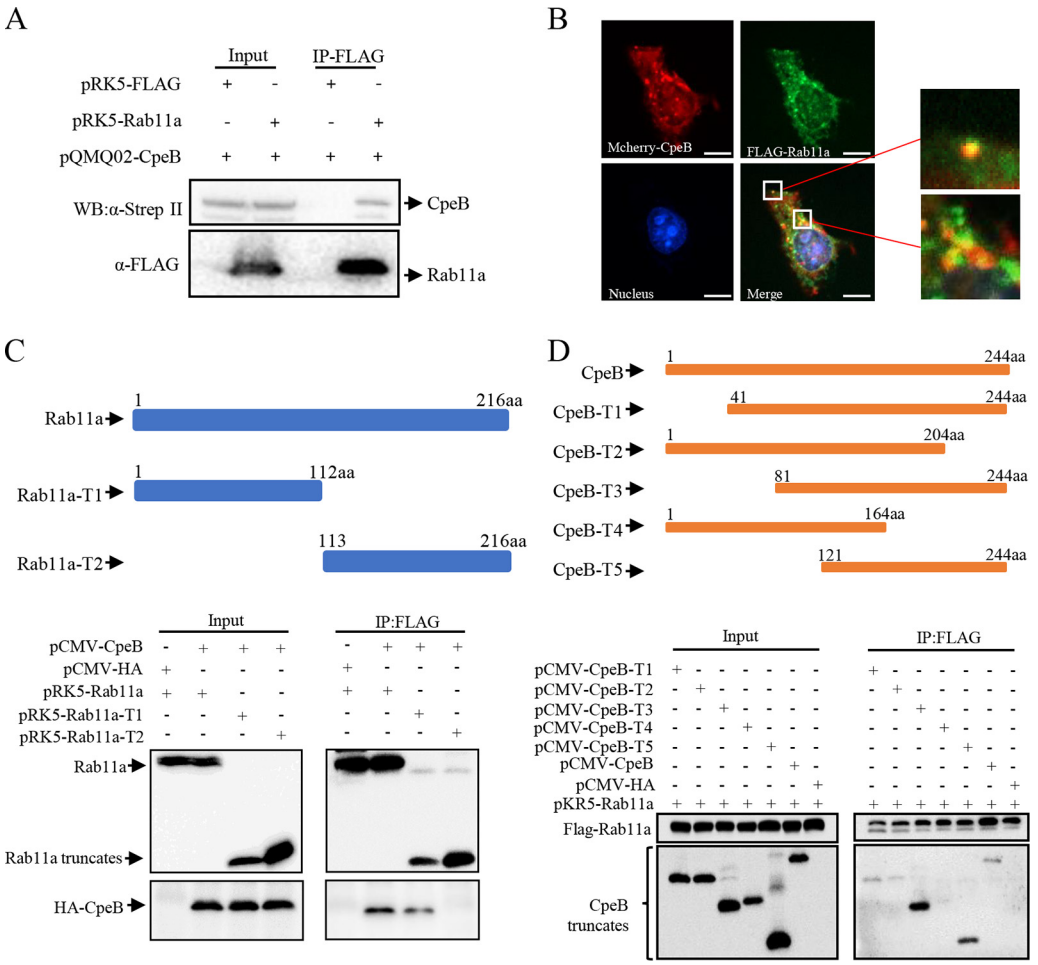

FIG 5 CpeB interacts with host Rab11a. (A) HeLa cells were transfected with the indicated expression plasmids. Twenty-four hours later, cells were lysed, and cell lysates were prepared for immunoprecipitation with anti-FLAG antibody and immunoblotted with anti-FLAG or anti-Strep-II antibodies. (B) HeLa cells coexpressing mCherry-CpeB and FLAG-Rab11a were fixed and probed with anti-FLAG antibody, followed by goat-anti-mouse Alexa Fluor 488 antibody (green). Nuclei were stained with DAPI. The samples were observed under a Nikon Eclipse Ti microscope (magnification, ×600; bar, 10 μm). (C) pCMV-CpeB or pCMV-HA was cotransfected with plasmids expressing Rab11a or Rab11a truncations. The diagrams of the truncations are shown on the top panels. Twenty-four hours after transfection, cell lysates were prepared and immunoprecipitated with anti-FLAG antibody and immunoblotted with anti-FLAG or anti-HA antibodies. (D) FLAG-Rab11a and HA-CpeB truncations were ectopically coexpressed in HeLa cells. Twenty-four hours later, cell lysates were collected, and the interaction region was detected using co-IP as described above.

with Rab11a expression and found that, compared with that of the control group, the level of LC3-II induced by CpeB was reduced after Rab11a expression interference (Fig. 6G and Fig. S5C), suggesting that the effect of CpeB on inducing LC3-II accumulation partially depends on Rab11a.

The pathogenicity of *C. burnetii* decreases in Rab11a$^{-/-}$ CKO mice. Inhalation of infected aerosols is the main transmission route of *C. burnetii* (4), so the *C. burnetii* colonization in the lungs plays a vital role in the process of infection. Among the different types of cells in lung, alveolar macrophages are the preferred niches for *C. burnetii* replication (36, 37). Thus, the macrophage Rab11a conditional knockout mice (Rab11a$^{-/-}$ CKO) were generated to further explore the role of Rab11a in *C. burnetii* infection. After infection with *C. burnetii* (Henzerling phase I stain) via the intratracheal (i.t.) route, the splenomegaly of Rab11a$^{-/-}$ CKO mice was much less severe than that of WT mice (Fig. 7A). In accordance with the size of splenomegaly, the ratios of spleen weight to body weight and *C. burnetii* loads in spleens or lungs of Rab11a$^{-/-}$ CKO mice were also much lower than those of WT mice (Fig. 7B to D). Histopathological analysis showed that the inflammation and pathological changes in the lungs of Rab11a$^{-/-}$ CKO mice

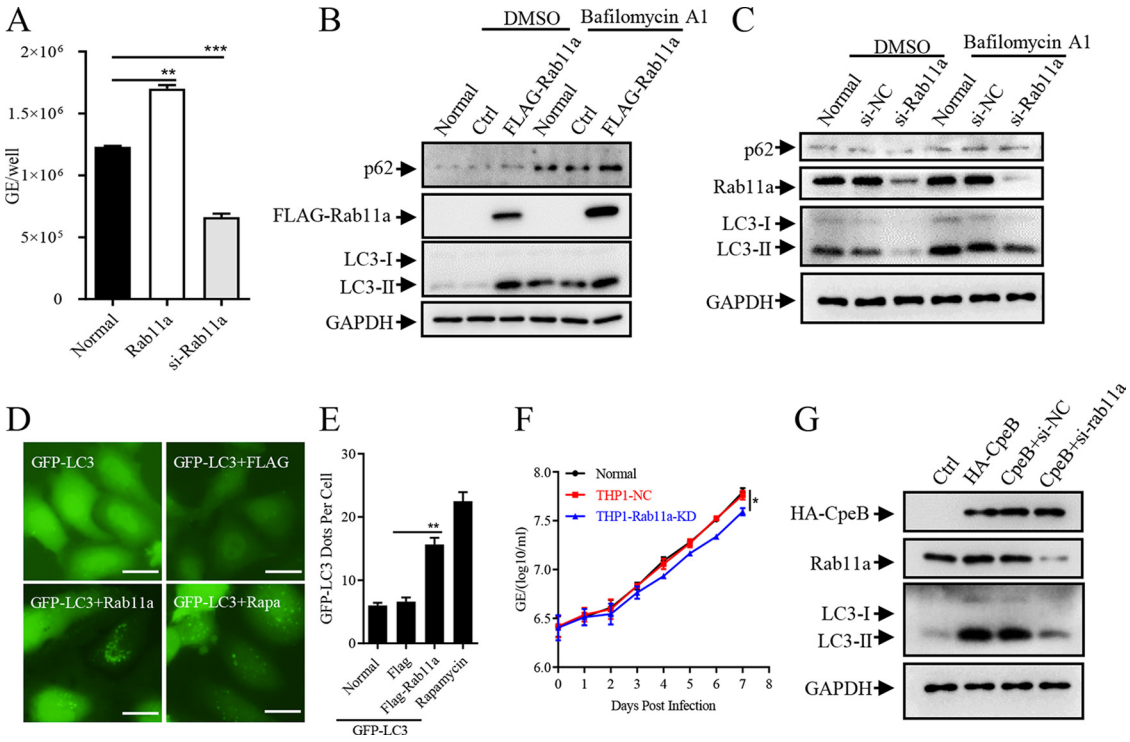

FIG 6 Rab11a affects the intracellular replication of *C. burnetii* through modulating autophagy. (A) HeLa cells were left untransfected (normal) or transfected with pRK5-Rab11a or si-rab11a. Twelve hours later, cells were infected with *C. burnetii* at an MOI of 100. Total DNA was extracted 4 days postinfection, and the copies of the *C. burnetii* genome were quantitated by qPCR. (B) HeLa cells were transfected with pRK5-Rab11a or control vectors, and cells were collected 24 h later with or without bafilomycin A1 pretreatment. The expression of LC3 and p62 was detected by Western blotting, and the expression of GAPDH was used as an internal control. (C) Si-Rab11a or siRNA control was transfected into HeLa cells, and the indicated proteins were detected 48 h later using Western blotting. (D) GFP-LC3 and FLAG-Rab11a or a control vector were coexpressed in HeLa cells, and the GFP-LC3 dots were observed under a fluorescence microscope (magnification, ×200; bar, 20 μm) 24 h later. (E) The numbers of GFP-LC3 dots per cell (n = 20) were counted. Data are representative of three independent experiments, and bars represent the mean ± SD of three independent experiments. **, $P < 0.01$. (F) THP-1, THP1-NC, or THP1-Rab11a-KD cells were infected with *C. burnetii*. The samples were collected daily, and the genome equivalents of *C. burnetii* were determined by qPCR. Experiments were repeated three times independently, and the trend was consistent. Data are representative of three independent experiments, and bars represent the mean ± SD from three independent experiments. *, $P < 0.05$. (G) CpeB was separately transfected or cotransfected with si-Rab11a into HeLa cells. Thirty-six hours later, cells with bafilomycin A1 pretreatment were lysed, and cell lysates were subjected to Western blotting. The expression of CpeB, Rab11a, and LC3 was detected using indicated antibodies, and GAPDH was used as an internal control.

were milder, mainly manifested as less lymphocyte infiltration around the bronchi and blood vessels and more complete alveolar structure than those of wild-type mice. Meanwhile, the alveolar structure of WT mice was destroyed; however, the alveolar walls of Rab11a$^{-/-}$ CKO mice remained intact, and the number of lymphocytes in the lungs of Rab11a$^{-/-}$ CKO mice was much lower than that of WT mice (Fig. 7E). Taken together, these results demonstrated that Rab11a deficiency in macrophages inhibits *C. burnetii* replication in host cells.

DISCUSSION

The ability of *C. burnetii* to grow and replicate in lysosome-derived acidic vacuoles after invading host cells has raised many questions by researchers (16, 38). With the development of axenic growth, genetic mechanistic methodology, and infection models (35, 39, 40), the underlying mechanism of pathogen-host interaction of *C. burnetii* has been gradually uncovered. Here, we showed that the effector protein CpeB encoded by QpH1 plasmid is involved in inducing LC3-II accumulation during *C. burnetii* infection.

CpeB is an effector protein encoded by all *C. burnetii* plasmids. Early studies demonstrated that CpeB is highly expressed during the rapid expansion period of CCVs at 2 and 3 days postinfection and colocalizes with LC3 (29). In our study, *C. burnetii* infection or

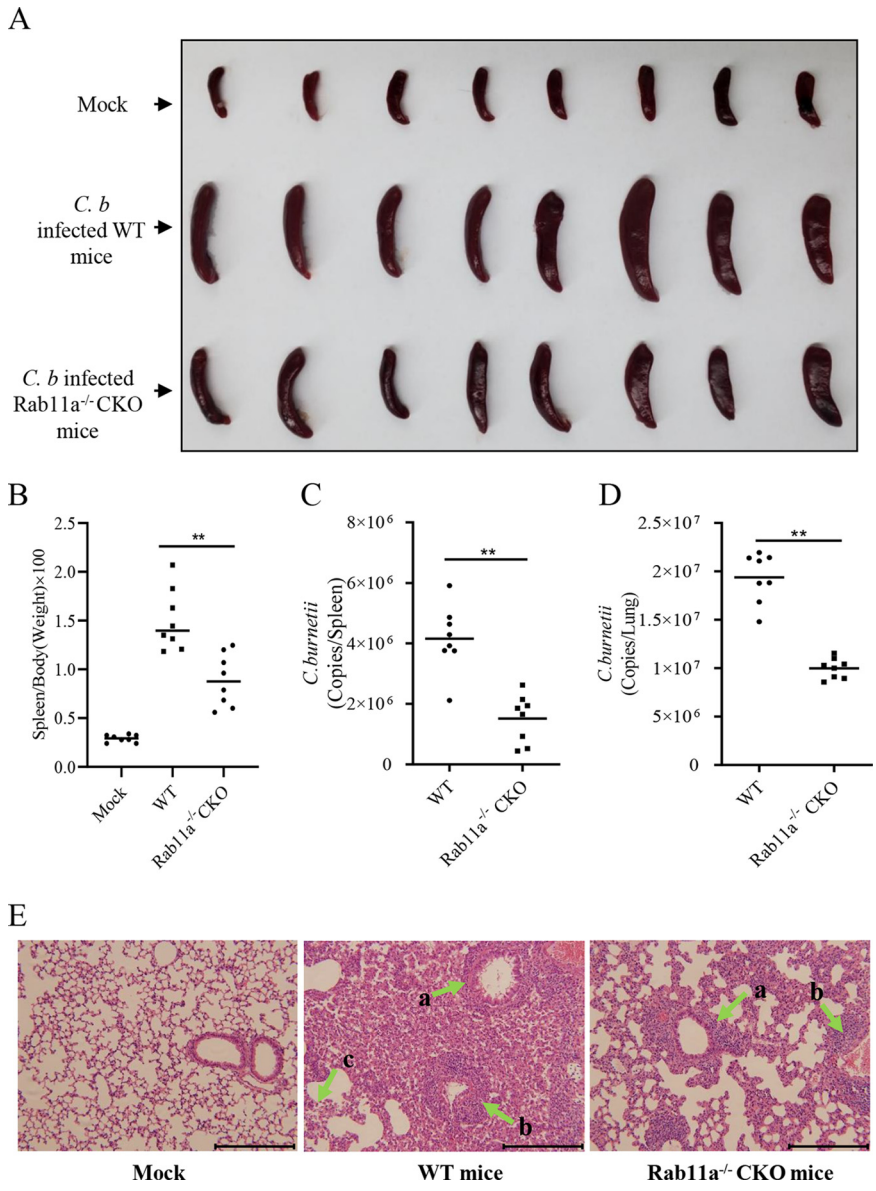

FIG 7 The pathogenicity of *C. burnetii* decreased in Rab11a$^{-/-}$ CKO mice. (A) Mock-infected mice, WT *C. burnetii*-infected C57BL/6J WT mice, or Rab11a$^{-/-}$ CKO mice were sacrificed at 14 days postinfection. The spleens of the mice were removed and photographed after bloodletting. (B) The ratio of spleen weight to body weight of each mouse was calculated. (C and D) The spleens (C) or lungs (D) of the WT or Rab11a$^{-/-}$ CKO mice were ground, and the genome copies of *C. burnetii* were determined by qPCR. The data are presented as the mean of $n = 8$ mice per group, and the standard error is indicated by the error bar. (E) The lungs of mice were fixed in formalin, and the pathological lesions were observed in hematoxylin and eosin (H&E)-stained sections under a light microscope. Chronic lymphocyte infiltration around the bronchi (arrow a), chronic lymphocyte infiltration around blood vessels (arrow b), and plasmacytes (arrow c) were observed in the lungs of mice (magnification, ×400; bar, 100 μm).

ectopic expression of CpeB induced increased levels of LC3-II and the stabilized levels of p62, which was consistent with previous results (41). However, compared with NMII, expression of CpeB in the QpH1-deficient strain restored the LC3-II content only until day 4 postinfection. Even though the LC3-II content in NMII*pQGK-cpeB*-infected cells was much higher than that in NMII*pQGK*-infected cells, it was much less than that in NMII-infected cells at day 5 and day 6 postinfection. This result indicated that CpeB largely restored the decrease in LC3-II levels caused by QpH1 deficiency, but there might be other effector proteins that played a role in the maintenance of high LC3 levels in the late stage of *C. burnetii* infection. Besides CpeB, the *C. burnetii* effectors CvpB, CvpF, and Cig57 have also been reported to be

involved in the manipulation of host autophagy, highlighting the importance of this pathway to CCV biogenesis (42). Meanwhile, LC3 was still decorated on CCVs generated by NMII*pQGK* lacking CpeB, indicating that CpeB might not be necessary for LC3 recruitment to the CCVs (see Fig. S4A and B in the supplemental material). Additionally, small vacuoles were observed in host cells infected with QpH1-deficient strains, and this phenotype could not be rescued by the expression of CpeA, CpeB, or CpeC in QpH1-deficient strains. As reported in numerous studies, loss of function in one of the essential T4SS effectors could lead to the formation of small CCVs in macrophage-like cells (43). Therefore, it was reasonable to assume that other effectors encoded by QpH1 might contribute to the homotypic fusion of CCVs.

Several proteins have been confirmed to be *C. burnetii* virulence factors in infected cells, including the essential factors of theT4SS (9, 44) and the effectors Cir (45), Cvp (46), and Ank (47). Recently, the identification of virulence determinators encoded by QpH1 plasmid has been greatly facilitated by the incompatible plasmid-curing approach (48). Using this approach, we found that the expression of CpeB in a plasmid-deficient strain could partially complement the pathogenetic defect of the QpH1-deficient strain in SCID mice, inducing a higher bacterial burden in organs of the infected mice. However, the role of CpeB in bacterial virulence and modulation of autophagy need to be further verified with the *cpeB* single-gene deletion strain by using the method reported by Beare et al. (49, 50).

Rab11a was identified as the host target of CpeB, and the interaction had been verified as described above, but the underlying mechanism of this interaction had not been clarified. We first investigated whether CpeB influences the expression of endogenous Rab11a; however, the results showed that ectopically expressed CpeB has no effect on the expression of Rab11a compared to the control in HeLa and HEK-293T cells (Fig. S6A). The activation of Rab11a is controlled by reversible binding to GTP or GDP, and this process is regulated by multiple molecules, the most important of which are two families of proteins, GAPs and guanine nucleotide exchange factors (GEFs) (51–53). Thus, we detected the intrinsic activity of prokaryotically expressed Rab11a and the potential role of CpeB in modulating Rab11a activity. Using the GTPase-Glo assay, we confirmed that recombinant expressed Rab11a possessed low GTPase activity (Fig. S6B), and CpeB had no significant effect on the enzyme activity of Rab11a (Fig. S6C and D), indicating that CpeB might be neither a GEF nor a GAP for Rab11a. But this result would be further confirmed by the presence of a known GEF or GAP of Rab11a, such as Crag (54) or C9ORF72-SMCR8 complex (55). Nevertheless, this result also gave us some hints that CpeB might affect Rab11a in other ways, such as preferentially binding to active Rab11a or inactive Rab11a or influencing the combination of Rab11a and Rab11 family-interacting proteins (FIPs).

In conclusion, we showed that *C. burnetii* effector protein CpeB interacts with autophagy-related protein Rab11a, and we verified the promotion of LC3-II accumulation by CpeB in host cells. Additionally, CpeB is a potential *C. burnetii* virulence factor because of its enhancement of *C. burnetii* pathogenicity in a SCID mouse model. Infection of Rab11a$^{-/-}$ CKO mice also verified that the host Rab11a protein is capable of promoting *C. burnetii* infection in mice. Our work will help broaden the understanding of the role of autophagy in *C. burnetii* infection and provide new references for identifying *C. burnetii* virulence factors.

MATERIALS AND METHODS

Cell lines, bacterial strains, and mice. Human embryonic kidney cells (HEK293T), human cervical cancer cells (HeLa), and sp2/0 myeloma cells were purchased from ATCC and maintained in Dulbecco's modified Eagle medium (DMEM) containing 10% fetal bovine serum (FBS). Human monocytic leukemia cells (THP-1) were also obtained from ATCC and cultured in RPMI 1640 medium supplemented with 10% FBS and 0.1% 2-mercaptoethanol (Gibco; catalog no. 21985023). THP1-CpeB (a stable cell line expressing CpeB), THP1-Rab11a (a stable cell line expressing Rab11a), THP1-Rab11a-KD (a stable Rab11a knockdown cell line), and THP1-NC (an empty lentivirus transduced cell line) were constructed by GenePharma (Suzhou, China) and cultured in RPMI 1640 medium with 10% FBS and 0.1% 2-mercaptoethanol as well as 1 μg/mL puromycin (Sigma; catalog no. 540411). For the THP1-CpeB and THP1-Rab11a cell lines, the

cpeB or *rab11a* gene was cloned into the region downstream of the *EF1a* promoter in a lentivirus shuttle plasmid. For the THP1-Rab11a-KD cell line, siRNA targeting *rab11a* (5′-TGT CAG ACA GAC GCG AAA ATT-3′) was inserted into the downstream region of the U6 promoter in a lentivirus shuttle plasmid. All cell lines were cultured at 37°C in 5% CO_2. The *Coxiella burnetii* Nine Mile RSA439 strain (phase II) and Henzerling strain (phase I) were cultivated in acidified citrate cysteine medium-2 (ACCM-2) in 5% CO_2 and 2.5% O_2 at 37°C as previously described (56). Severe combined immune deficiency (SCID) mice and C57BL/6J mice (aged 6 to 8 weeks) were purchased from Vital River Laboratories (Beijing, China). Macrophage Rab11a conditional knockout (Rab11a$^{-/-}$ CKO) mice were generated by Cyagen Biosciences Inc. (Guangzhou, China).

Generation of *C. burnetii* mutants. QpH1-based shuttle plasmids were constructed by cloning the kanamycin resistance (Kan^r) cassette, enhanced green fluorescent protein (eGFP), and the *cbua0036-0039a* gene into the RSF1010 ori-based vector pQGK as previously described (48). Then, the coding sequences of *cpeA*, *cpeB*, and *cpeC* were cloned downstream of the P1169 promoter on pQGK by homologous recombination to generate the pQGK-CpeA, pQGK-CpeB, and pQGK-CpeC shuttle plasmids, respectively. The plasmid map is provided in Fig. S1 in the supplemental material. For the generation of QpH1-deficient mutants, approximately 20 μg of pQGK-based shuttle vectors were electroporated into *C. burnetii* Nine Mile phase II strain with the electroporation conditions of 1.8 kV, 25 μF, and 500 Ω as previously described (39). After 3 passages in ACCM-2 with kanamycin (400 μg/mL), positive *C. burnetii* transformants were screened using ACCM-2 agar plates with kanamycin. Using an optical microscope, individual *C. burnetii* colonies with clear boundaries and fluorescence were marked, and then, each colony was removed and placed into individual wells of a 96-well plate with 100 μL of fresh ACCM-2. After 3 passages, 1 mL of the transformed bacteria was pelleted to extract genomic DNA. The QpH1-deficient strain of *C. burnetii* (NMII*pQGK*) and the expression of Cpes in NMII*pQGK* (NMII*pQGK-cpe*) mutants were verified by qRT-PCR with primers specific for the deleted or introduced *cpe* genes and the primers specific for *cbua0036* as a control.

***C. burnetii* growth in bacteriological medium and cells.** *C. burnetii* wild-type (WT) or mutant strains were cultivated in ACCM-2 with or without the presence of antibiotics. To assess the growth characteristics, *C. burnetii* strains were inoculated into 20 mL of fresh ACCM-2 at a concentration of 1×10^6 genome equivalents (GEs)/mL. At different time points (1, 2, 3, 4, 5, 6, and 7 days) postinoculation, 1 mL of each sample was taken for DNA extraction. The *C. burnetii* GE was quantitated by qPCR targeting the *com*1 gene as previously described (57). For host cell infection, HeLa cells were seeded in 12-well plates at 2×10^5 cells per well and cultured in DMEM medium containing 1% fetal bovine serum (FBS), and then, the cells were infected with *C. burnetii* at a multiplicity of infection (MOI) of 100. THP-1 cells (1×10^6 cells/well) were differentiated into macrophage-like cells by phorbol myristate acetate (Sigma; catalog no. p8139) at 200 nM and then infected with *C. burnetii* at an MOI of 10 after cell adhesion. Six hours postinfection, the cells were washed twice with phosphate-buffered saline (PBS) and continually incubated in fresh medium for the indicated times before cell collection for different experiments. To detect the effect of autophagy on *C. burnetii* replication, the infected THP-1 cells were cultured in fresh medium with rapamycin (Abcam; catalog no. ab120224) at different concentrations or stimulated with bafilomycin A1 (Sigma; catalog no. 19-148) for 6 h every 48 h. Genomic DNA from *C. burnetii*-infected cells was extracted, and genome copy numbers were determined by a probe specific to *com*1.

Animal experiments. SCID mice were randomly divided into 3 groups (7 mice per group) and were infected with the *C. burnetii* wild-type strain (Nine Mile phase II [NMII]), NMII*pQGK*, or NMII*pQGK-cpeB* mutant (2×10^6 GE per mouse) via intraperitoneal (i.p.) injection, respectively. Two weeks postinfection, the mice were sacrificed. The body and spleen of each mouse were weighed, and genomic DNA was extracted from each organ. To determine GEs per sample, qRCR was performed with primers specific for the *com*1 gene. Additionally, C57BL/6J wild-type mice or Rab11a$^{-/-}$ CKO mice were infected with *C. burnetii* Henzerling strain (phase I strain) at the dose of 1×10^7 GE per mouse via intratracheal (i.t.) inoculation as previously described (58). Mice were sacrificed at 2 weeks postinfection. The lungs of each mouse were removed and immediately fixed in formalin for preparation of pathological slices. The spleens and liver of each mouse were weighed, and bacterial burden in each organ was determined by qPCR.

Generation of anti-CpeB monoclonal antibody. Prokaryotically expressed His-CpeB proteins (30 μg) and complete Freund's adjuvant (Sigma; catalog no. F5881) of equal volume were emulsified until a thickened mixture resulted. Female BALB/c mice (6 to 8 weeks) were injected subcutaneously with the emulsion at a dose of 0.1 mL/mouse and boosted at intervals of 14 days with approximately the same dose of antigen emulsified in incomplete Freund's adjuvant (Sigma; catalog no. F5506) twice. Then, the immunized mice were sacrificed, and the spleens were harvested. After lysing red blood cells and resuspension, spleen cells and sp2/0 myeloma cells were mixed and fused in the presence of 50% polyethylene glycol (PEG). The primary hybridoma was screened by enzyme-linked immunosorbent assay (ELISA), and positive monoclonal hybridoma lines were established by limiting dilution. After three generations of clones by limiting dilution, stable monoclonal antibody-producing hybridoma lines were obtained and injected into mice intraperitoneally with 5×10^6 cells/mouse to produce ascites fluid. One to 2 weeks later, ascites samples were harvested, and the anti-CpeB monoclonal antibody was purified with saturated ammonium sulfate.

Affinity purification-mass spectrometry. The coding sequence of *cpeB* was cloned into pQM02 with a C-terminal twin Strep-II tag and an N-terminal mCherry tag. The eukaryotic expression plasmid pQM02-CpeB or pQM02 control plasmid was transfected into HEK-293T cells using Lipofectamine 3000 (Invitrogen; catalog no. L3000001). Cells were lysed with lysis buffer (100 mM Tris-HCl, pH 8.0, 150 mM NaCl, 1 mM EDTA, and 1% NP-40) with complete EDTA-free protease and PhosStop phosphatase inhibitor cocktails 36 h posttransfection, and cell lysates were incubated with Strep-Tactin Sepharose beads (GE; catalog no. 28-9355-99) at room temperature for 1 h. Then, the Strep-Tactin beads were washed

with lysis buffer 6 times before being eluted with lysis buffer containing 2.5 mM D-desthiobiotin. Each eluate was quantitated using a bicinchoninic acid (BCA) protein assay kit, and the purification and enrichment of Strep-CpeB were estimated by Western blotting. At least 3 independent replicates were performed for the expression and purification of each protein. Each purified protein (~100 μg) was freeze-dried, digested, and desalted for liquid chromatography-mass spectrometry (LC-MS).

Coimmunoprecipitation. CpeB and its truncations were cloned into the indicated plasmids, and Rab11a and its truncations were cloned into pRK5-FLAG with an N-terminal FLAG tag. HeLa cells were cotransfected with plasmids overexpressing CpeB or Rab11a or empty vector as controls using Lipofectamine 3000. Twenty-four hours after transfection, cells were lysed using radioimmunoprecipitation assay (RIPA) lysis buffer with protease and phosphatase inhibitor cocktails on ice for 20 min. After centrifugation at 6,000 rpm for 20 min to remove the debris, cell lysates were incubated with 1 μg of anti-FLAG antibody (Sigma; catalog no. F1804) and 50 μL of GammaBind G Sepharose beads (GE; catalog no. 17061801) at 4°C overnight. The beads were washed 6 times with RIPA buffer at 3,000 rpm and 4°C and boiled with 2× SDS loading buffer of the same volume for 10 min. The samples were analyzed by Western blotting using anti-FLAG, anti-hemagglutinin (HA) (Abcam; catalog no. ab9110), or anti-Strep-II (MBL; catalog no. M112-3) antibodies, followed by an appropriate secondary antibody.

Confocal microscopy assay. HeLa cells were seeded on coverslips in 24-well plates and transfected with 1 μg of the indicated plasmids using Lipofectamine 3000. Twenty-four hours posttransfection, the cells were fixed with 4% paraformaldehyde and permeabilized with 0.2% Triton X-100 for 15 min at room temperature. Permeabilized cells were blocked with 1% bovine serum albumin for 30 min and probed with anti-FLAG, anti-HA, anti-LC3-II (CST; catalog no. 3868S), or anti-LAMP1 (CST; catalog no. 9091S) antibody, followed by goat anti-mouse IgG Alexa Fluor 488 antibody (Abcam; catalog no. ab150113) or goat anti-rabbit IgG Alexa Fluor 594 antibody (Abcam; catalog no. ab150116). Finally, the cells were incubated with DAPI (4′,6-diamidino-2-phenylindole) for 1 min to stain the nuclei. Coverslips were mounted on slides with Prolong Gold antifade mounting solution (Thermo Fisher; catalog no. p36935). Samples were observed with a spinning disk confocal microscope (Nikon Eclipse Ti microscope). To access the subcellular localization of CpeB during *C. burnetii* infection, THP-1 cells were seeded onto coverslips in 24-well plates in the presence of 200 nM phorbol myristate acetate (PMA). Two days later, cells were infected with *C. burnetii* at an MOI of 10. Four days after infection, the cell culture medium was discarded, and the cells were washed 3 times with precooled PBS. Then, the cells were fixed and blocked as described above. Next, mouse anti-*C. burnetii* serum, mouse anti-CpeB antibody, or rabbit anti-LAMP1 antibody was used as primary antibody. After staining with secondary antibodies and DAPI, confocal images were obtained with the confocal microscope.

Western blotting. Protein samples were fractionated by electrophoresis on 10% SDS-PAGE gels, and resolved proteins were transferred to polyvinylidene difluoride (PVDF) membranes. After blocking with 5% skim milk, the membranes were incubated with the indicated primary antibodies, followed by appropriate horseradish peroxidase (HRP)-conjugated secondary antibodies. For analysis of autophagy, cells were transfected with the indicated plasmids in the presence or absence of 50 nM bafilomycin A1 or infected with different *C. burnetii* strains. Then, the cells were lysed and subjected to Western blotting using anti-LC3 (CST; catalog no. 3868S), anti-p62 (CST; catalog no. 8588S), anti-Rab11a (Thermo Fisher; catalog no. 71-5300), or anti-GAPDH (glyceraldehyde-3-phosphate dehydrogenase) (Proteintech; catalog no. 60004-1) antibodies followed by HRP-conjugated goat anti-mouse antibodies (Gene-Protein; catalog no. p03S01) or HRP-conjugated goat anti-rabbit antibodies (Gene-Protein; catalog no. p03S02). Blots were visualized using an ECL kit.

GTPase activity assay. The experiment was carried out using the GTPase-Glo assay kit (Promega; catalog no. V7681). Briefly, for detection of the GTPase activity of Rab11a, 25 μL of GTPase/GAP (GTPase-activating proteins) buffer containing Rab11a at different concentrations, 5 or 2 μM GTP, and 1 mM dithiothreitol (DTT) was added to each well in a solid white 96-well plate. For analysis of the potential GAP or GEF activity of CpeB, 25 μL of GAP or GEF buffer containing 4 μM Rab11a, 1 mM DTT, 5 μM GTP, and different concentrations of purified CpeB were added to each well. The control group was set up at the same time. After incubation at room temperature for 90 min, 25 μL of prepared 1 mL reaction solution with 2 μL of GTPase-Glo 500 reagent, 0.5 μL of ADP and 998 μL of GTPase-Glo buffer was added to each well in the 96-well plate. Then, the plate was incubated with shaking for 30 min before 50 μL of detection reagent was added, and the full-wavelength luminescence was measured after 5 to 10 min of incubation.

Study approval. Infectious experiments with *C. burnetii* phase I strain were conducted in the animal biosafety level 3 laboratory (ABSL3) and carried out according to the guidelines of the authors' institution. All procedures for animal experiments were approved by the Institute of Animal Care and Use Committee (IACUC) of the Academy of Military Medical Sciences (approval no. IACUC-DWZX-2020-003), and all experiments were performed in accordance with the regulation and guidelines of this committee.

Statistical analysis. Statistical significance of *C. burnetii* GE, band density, ratio of spleen or liver weight to body weight, and splenomegaly data were determined by Student's *t* test or one-way analysis of variance (ANOVA). Data were analyzed using GraphPad Prism 8.0 software (GraphPad). For all analyses, a P value of <0.05 was deemed significant.

SUPPLEMENTAL MATERIAL

Supplemental material is available online only.

SUPPLEMENTAL FILE 1, PDF file, 0.4 MB.

SUPPLEMENTAL FILE 2, XLSX file, 0.1 MB.

ACKNOWLEDGMENTS

This work was supported by grants from the National Natural Science Foundation of China, numbers 32000140 and 31970178.

We declared that the research was conducted in the absence of any commercial or financial relationships that could be construed as a potential conflict of interest.

X.X., J.J., and M.F. designed and conceived the experiments, conducted the data analysis, and wrote and revised the manuscript. M.F. and J.Z. mainly performed the experiments. M.Z., S.Z., and L.D. contributed and shared some experimental materials, reagents, and instruments. Y.Y. and X.O. conducted the formal analysis. B.W., Y.S., and D.Z. revised and edited the manuscript.

REFERENCES

1. Schneeberger PM, Wintenberger C, van der Hoek W, Stahl JP. 2014. Q fever in the Netherlands–2007–2010: what we learned from the largest outbreak ever. Med Mal Infect 44:339–353. https://doi.org/10.1016/j.medmal.2014.02.006.
2. van Schaik EJ, Chen C, Mertens K, Weber MM, Samuel JE. 2013. Molecular pathogenesis of the obligate intracellular bacterium Coxiella burnetii. Nat Rev Microbiol 11:561–573. https://doi.org/10.1038/nrmicro3049.
3. Oyston PCF, Davies C. 2011. Q fever: the neglected biothreat agent. J Med Microbiol 60:9–21. https://doi.org/10.1099/jmm.0.024778-0.
4. Parker NR, Barralet JH, Bell AM. 2006. Q fever. Lancet 367:679–688. https://doi.org/10.1016/S0140-6736(06)68266-4.
5. Dragan AL, Voth DE. 2020. Coxiella burnetii: international pathogen of mystery. Microbes Infect 22:100–110. https://doi.org/10.1016/j.micinf.2019.09.001.
6. Kohler LJ, Roy CR. 2015. Biogenesis of the lysosome-derived vacuole containing Coxiella burnetii. Microbes Infect 17:766–771. https://doi.org/10.1016/j.micinf.2015.08.006.
7. Qiu J, Luo ZQ. 2017. Legionella and Coxiella effectors: strength in diversity and activity. Nat Rev Microbiol 15:591–605. https://doi.org/10.1038/nrmicro.2017.67.
8. Howe D, Shannon JG, Winfree S, Dorward DW, Heinzen RA. 2010. Coxiella burnetii phase I and II variants replicate with similar kinetics in degradative phagolysosome-like compartments of human macrophages. Infect Immun 78:3465–3474. https://doi.org/10.1128/IAI.00406-10.
9. Carey KL, Newton HJ, Luhrmann A, Roy CR. 2011. The Coxiella burnetii Dot/Icm system delivers a unique repertoire of type IV effectors into host cells and is required for intracellular replication. PLoS Pathog 7:e1002056. https://doi.org/10.1371/journal.ppat.1002056.
10. Chen C, Banga S, Mertens K, Weber MM, Gorbaslieva I, Tan Y, Luo ZQ, Samuel JE. 2010. Large-scale identification and translocation of type IV secretion substrates by Coxiella burnetii. Proc Natl Acad Sci U S A 107:21755–21760. https://doi.org/10.1073/pnas.1010485107.
11. Lifshitz Z, Burstein D, Peeri M, Zusman T, Schwartz K, Shuman HA, Pupko T, Segal G. 2013. Computational modeling and experimental validation of the Legionella and Coxiella virulence-related type-IVB secretion signal. Proc Natl Acad Sci U S A 110:E707–E715. https://doi.org/10.1073/pnas.1215278110.
12. Larson CL, Martinez E, Beare PA, Jeffrey B, Heinzen RA, Bonazzi M. 2016. Right on Q: genetics begin to unravel Coxiella burnetii host cell interactions. Future Microbiol 11:919–939. https://doi.org/10.2217/fmb-2016-0044.
13. Latomanski EA, Newton HJ. 2018. Interaction between autophagic vesicles and the Coxiella-containing vacuole requires CLTC (clathrin heavy chain). Autophagy 14:1710–1725. https://doi.org/10.1080/15548627.2018.1483806.
14. Larson CL, Sandoz KM, Cockrell DC, Heinzen RA. 2019. Noncanonical inhibition of mTORC1 by Coxiella burnetii promotes replication within a phagolysosome-like vacuole. mBio 10:e02816-18. https://doi.org/10.1128/mBio.02816-18.
15. Gutierrez MG, Vazquez CL, Munafo DB, Zoppino FC, Beron W, Rabinovitch M, Colombo MI. 2005. Autophagy induction favours the generation and maturation of the Coxiella-replicative vacuoles. Cell Microbiol 7:981–993. https://doi.org/10.1111/j.1462-5822.2005.00527.x.
16. Winchell CG, Graham JG, Kurten RC, Voth DE. 2014. Coxiella burnetii type IV secretion-dependent recruitment of macrophage autophagosomes. Infect Immun 82:2229–2238. https://doi.org/10.1128/IAI.01236-13.
17. Romano PS, Gutierrez MG, Beron W, Rabinovitch M, Colombo MI. 2007. The autophagic pathway is actively modulated by phase II Coxiella burnetii to efficiently replicate in the host cell. Cell Microbiol 9:891–909. https://doi.org/10.1111/j.1462-5822.2006.00838.x.
18. Newton HJ, Kohler LJ, McDonough JA, Temoche-Diaz M, Crabill E, Hartland EL, Roy CR. 2014. A screen of Coxiella burnetii mutants reveals important roles for Dot/Icm effectors and host autophagy in vacuole biogenesis. PLoS Pathog 10:e1004286. https://doi.org/10.1371/journal.ppat.1004286.
19. Martinez E, Allombert J, Cantet F, Lakhani A, Yandrapalli N, Neyret A, Norville IH, Favard C, Muriaux D, Bonazzi M. 2016. Coxiella burnetii effector CvpB modulates phosphoinositide metabolism for optimal vacuole development. Proc Natl Acad Sci U S A 113:E3260–E3269. https://doi.org/10.1073/pnas.1522811113.
20. Stein MP, Muller MP, Wandinger-Ness A. 2012. Bacterial pathogens commandeer Rab GTPases to establish intracellular niches. Traffic 13:1565–1588. https://doi.org/10.1111/tra.12000.
21. Newton HJ, McDonough JA, Roy CR. 2013. Effector protein translocation by the Coxiella burnetii Dot/Icm type IV secretion system requires endocytic maturation of the pathogen-occupied vacuole. PLoS One 8:e54566. https://doi.org/10.1371/journal.pone.0054566.
22. Rejman Lipinski A, Heymann J, Meissner C, Karlas A, Brinkmann V, Meyer TF, Heuer D. 2009. Rab6 and Rab11 regulate Chlamydia trachomatis development and golgin-84-dependent Golgi fragmentation. PLoS Pathog 5:e1000615. https://doi.org/10.1371/journal.ppat.1000615.
23. Siadous FA, Cantet F, Van Schaik E, Burette M, Allombert J, Lakhani A, Bonaventure B, Goujon C, Samuel J, Bonazzi M, Martinez E. 2021. Coxiella effector protein CvpF subverts RAB26-dependent autophagy to promote vacuole biogenesis and virulence. Autophagy 17:706–722. https://doi.org/10.1080/15548627.2020.1728098.
24. Puri C, Vicinanza M, Ashkenazi A, Gratian MJ, Zhang Q, Bento CF, Renna M, Menzies FM, Rubinsztein DC. 2018. The RAB11A-positive compartment is a primary platform for autophagosome assembly mediated by WIPI2 recognition of PI3P-RAB11A. Dev Cell 45:114–131.e8. https://doi.org/10.1016/j.devcel.2018.03.008.
25. Ning Z, Yu SR, Quan YG, Xue Z. 1992. Molecular characterization of cloned variants of Coxiella burnetii isolated in China. Acta Virol 36:173–183.
26. Valkova D, Kazar J. 1995. A new plasmid (QpDV) common to Coxiella burnetii isolates associated with acute and chronic Q fever. FEMS Microbiol Lett 125:275–280. https://doi.org/10.1111/j.1574-6968.1995.tb07368.x.
27. Lautenschlager S, Willems H, Jager C, Baljer G. 2000. Sequencing and characterization of the cryptic plasmid QpRS from Coxiella burnetii. Plasmid 44:85–88. https://doi.org/10.1006/plas.2000.1470.
28. Jager C, Lautenschlager S, Willems H, Baljer G. 2002. Coxiella burnetii plasmid types QpDG and QpH1 are closely related and likely identical. Vet Microbiol 89:161–166. https://doi.org/10.1016/s0378-1135(02)00155-4.
29. Voth DE, Beare PA, Howe D, Sharma UM, Samoilis G, Cockrell DC, Omsland A, Heinzen RA. 2011. The Coxiella burnetii cryptic plasmid is enriched in genes encoding type IV secretion system substrates. J Bacteriol 193:1493–1503. https://doi.org/10.1128/JB.01359-10.
30. Roman MJ, Crissman HA, Samsonoff WA, Hechemy KE, Baca OG. 1991. Analysis of Coxiella burnetii isolates in cell culture and the expression of parasite-specific antigens on the host membrane surface. Acta Virol 35:503–510.
31. Howe D, Melnicakova J, Barak I, Heinzen RA. 2003. Maturation of the Coxiella burnetii parasitophorous vacuole requires bacterial protein synthesis but not replication. Cell Microbiol 5:469–480. https://doi.org/10.1046/j.1462-5822.2003.00293.x.
32. Howe D, Melnicakova J, Barak I, Heinzen RA. 2003. Fusogenicity of the Coxiella burnetii parasitophorous vacuole. Ann N Y Acad Sci 990:556–562. https://doi.org/10.1111/j.1749-6632.2003.tb07426.x.
33. Bewley KR. 2013. Animal models of Q fever (Coxiella burnetii). Comp Med 63:469–476.

34. Andoh M, Zhang G, Russell-Lodrigue KE, Shive HR, Weeks BR, Samuel JE. 2007. T cells are essential for bacterial clearance, and gamma interferon, tumor necrosis factor alpha, and B cells are crucial for disease development in Coxiella burnetii infection in mice. Infect Immun 75:3245–3255. https://doi.org/10.1128/IAI.01767-06.
35. van Schaik EJ, Case ED, Martinez E, Bonazzi M, Samuel JE. 2017. The SCID mouse model for identifying virulence determinants in Coxiella burnetii. Front Cell Infect Microbiol 7:25. https://doi.org/10.3389/fcimb.2017.00025.
36. Graham JG, Winchell CG, Kurten RC, Voth DE. 2016. Development of an ex vivo tissue platform to study the human lung response to Coxiella burnetii. Infect Immun 84:1438–1445. https://doi.org/10.1128/IAI.00012-16.
37. Dragan AL, Kurten RC, Voth DE. 2019. Characterization of early stages of human alveolar infection by the Q fever agent Coxiella burnetii. Infect Immun 87:e00028-19. https://doi.org/10.1128/IAI.00028-19.
38. Kohler LJ, Reed Sh C, Sarraf SA, Arteaga DD, Newton HJ, Roy CR. 2016. Effector protein Cig2 decreases host tolerance of infection by directing constitutive fusion of autophagosomes with the Coxiella-containing vacuole. mBio 7:e01127-16. https://doi.org/10.1128/mBio.01127-16.
39. Beare PA, Heinzen RA. 2014. Gene inactivation in Coxiella burnetii. Methods Mol Biol 1197:329–345. https://doi.org/10.1007/978-1-4939-1261-2_19.
40. Sandoz KM, Beare PA, Cockrell DC, Heinzen RA. 2016. Complementation of arginine auxotrophy for genetic transformation of Coxiella burnetii by use of a defined axenic medium. Appl Environ Microbiol 82:3042–3051. https://doi.org/10.1128/AEM.00261-16.
41. Winchell CG, Dragan AL, Brann KR, Onyilagha FI, Kurten RC, Voth DE. 2018. Coxiella burnetii subverts p62/sequestosome 1 and activates Nrf2 signaling in human macrophages. Infect Immun 86:e00608-17. https://doi.org/10.1128/IAI.00608-17.
42. Thomas DR, Newton P, Lau N, Newton HJ. 2020. Interfering with autophagy: the opposing strategies deployed by Legionella pneumophila and Coxiella burnetii effector proteins. Front Cell Infect Microbiol 10:599762. https://doi.org/10.3389/fcimb.2020.599762.
43. Crabill E, Schofield WB, Newton HJ, Goodman AL, Roy CR. 2018. Dot/Icm-translocated proteins important for biogenesis of the Coxiella burnetii-containing vacuole identified by screening of an effector mutant sublibrary. Infect Immun 86:e00758-17. https://doi.org/10.1128/IAI.00758-17.
44. Beare PA, Gilk SD, Larson CL, Hill J, Stead CM, Omsland A, Cockrell DC, Howe D, Voth DE, Heinzen RA. 2011. Dot/Icm type IVB secretion system requirements for Coxiella burnetii growth in human macrophages. mBio 2:e00175-11. https://doi.org/10.1128/mBio.00175-11.
45. Weber MM, Chen C, Rowin K, Mertens K, Galvan G, Zhi H, Dealing CM, Roman VA, Banga S, Tan Y, Luo ZQ, Samuel JE. 2013. Identification of Coxiella burnetii type IV secretion substrates required for intracellular replication and Coxiella-containing vacuole formation. J Bacteriol 195:3914–3924. https://doi.org/10.1128/JB.00071-13.
46. Larson CL, Beare PA, Voth DE, Howe D, Cockrell DC, Bastidas RJ, Valdivia RH, Heinzen RA. 2015. Coxiella burnetii effector proteins that localize to the parasitophorous vacuole membrane promote intracellular replication. Infect Immun 83:661–670. https://doi.org/10.1128/IAI.02763-14.
47. Schafer W, Schmidt T, Cordsmeier A, Borges V, Beare PA, Pechstein J, Schulze-Luehrmann J, Holzinger J, Wagner N, Berens C, Heydel C, Gomes JP, Luhrmann A. 2020. The anti-apoptotic Coxiella burnetii effector protein AnkG is a strain specific virulence factor. Sci Rep 10:15396. https://doi.org/10.1038/s41598-020-72340-9.
48. Luo S, Lu S, Fan H, Sun Z, Hu Y, Li R, An X, Uversky VN, Chen Z, Tong Y, Song L. 2021. The Coxiella burnetii QpH1 plasmid is a virulence factor for colonizing bone marrow-derived murine macrophages. J Bacteriol 203:e00588-20. https://doi.org/10.1128/JB.00588-20.
49. Beare PA, Larson CL, Gilk SD, Heinzen RA. 2012. Two systems for targeted gene deletion in Coxiella burnetii. Appl Environ Microbiol 78:4580–4589. https://doi.org/10.1128/AEM.00881-12.
50. Beare PA, Jeffrey BM, Long CM, Martens CM, Heinzen RA. 2018. Genetic mechanisms of Coxiella burnetii lipopolysaccharide phase variation. PLoS Pathog 14:e1006922. https://doi.org/10.1371/journal.ppat.1006922.
51. Zhen Y, Stenmark H. 2015. Cellular functions of Rab GTPases at a glance. J Cell Sci 128:3171–3176. https://doi.org/10.1242/jcs.166074.
52. Nishino H, Saito T, Wei R, Takano T, Tsutsumi K, Taniguchi M, Ando K, Tomomura M, Fukuda M, Hisanaga SI. 2019. The LMTK1-TBC1D9B-Rab11A cascade regulates dendritic spine formation via endosome trafficking. J Neurosci 39:9491–9502. https://doi.org/10.1523/JNEUROSCI.3209-18.2019.
53. Del Villar SG, Voelker TL, Westhoff M, Reddy GR, Spooner HC, Navedo MF, Dickson EJ, Dixon RE. 2021. Beta-adrenergic control of sarcolemmal CaV1.2 abundance by small GTPase Rab proteins. Proc Natl Acad Sci U S A 118:e2017937118. https://doi.org/10.1073/pnas.2017937118.
54. Xiong B, Bayat V, Jaiswal M, Zhang K, Sandoval H, Charng WL, Li T, David G, Duraine L, Lin YQ, Neely GG, Yamamoto S, Bellen HJ. 2012. Crag is a GEF for Rab11 required for rhodopsin trafficking and maintenance of adult photoreceptor cells. PLoS Biol 10:e1001438. https://doi.org/10.1371/journal.pbio.1001438.
55. Tang D, Sheng J, Xu L, Zhan X, Liu J, Jiang H, Shu X, Liu X, Zhang T, Jiang L, Zhou C, Li W, Cheng W, Li Z, Wang K, Lu K, Yan C, Qi S. 2020. Cryo-EM structure of C9ORF72-SMCR8-WDR41 reveals the role as a GAP for Rab8a and Rab11a. Proc Natl Acad Sci U S A 117:9876–9883. https://doi.org/10.1073/pnas.2002110117.
56. Omsland A, Beare PA, Hill J, Cockrell DC, Howe D, Hansen B, Samuel JE, Heinzen RA. 2011. Isolation from animal tissue and genetic transformation of Coxiella burnetii are facilitated by an improved axenic growth medium. Appl Environ Microbiol 77:3720–3725. https://doi.org/10.1128/AEM.02826-10.
57. Huang M, Ma J, Jiao J, Li C, Chen L, Zhu Z, Ruan F, Xing L, Zheng X, Fu M, Ma B, Gan C, Mao Y, Zhang C, Sun P, Liu X, Lin Z, Chen L, Lu Z, Zhou D, Wen B, Chen W, Xiong X, Xia J. 2021. The epidemic of Q fever in 2018 to 2019 in Zhuhai city of China determined by metagenomic next-generation sequencing. PLoS Negl Trop Dis 15:e0009520. https://doi.org/10.1371/journal.pntd.0009520.
58. Feng J, Hu X, Fu M, Dai L, Yu Y, Luo W, Zhao Z, Lu Z, Du Z, Zhou D, Wen B, Jiao J, Xiong X. 2019. Enhanced protection against Q fever in BALB/c mice elicited by immunization of chloroform-methanol residue of Coxiella burnetii via intratracheal inoculation. Vaccine 37:6076–6084. https://doi.org/10.1016/j.vaccine.2019.08.041.